Journal of Photochemistry, 14 (1980) 1 - 10

STUDIES OF EXCITED STATE ABSORPTION OF THE DYE *p*-PHENYLENE-BIS-(5-PHENYL-2-OXAZOLE) IN LIQUID SOLUTION AND IN THE VAPOUR PHASE

G. MAROWSKY

Max-Planck-Institut für biophysikalische Chemie, Abteilung Laserphysik, D-3400 Göttingen (F.R.G.)

H. SCHOMBURG

Universität Essen-GHS, FB 7-Physik, D-4300 Essen 1 (F.R.G.)

(Received October 8, 1979; in revised form February 4, 1980)

Summary

Excited state absorption spectra of *p*-phenylene-bis-(5-phenyl-2-oxazole) (POPOP) in dioxan solution were obtained over a broad spectral range from 310 to 760 nm, which includes both the ground state absorption and the fluorescence regions. For POPOP in the vapour phase data for excited state absorption coefficients were measured by an analysis of the dependence of the amplified spontaneous emission on the pump intensity. In the fluorescence spectral range the cross sections for excited state absorption do not exceed 0.7×10^{-16} cm^2 for both POPOP vapour and POPOP in liquid solution.

1. Introduction

The influence of the absorption of both pump light and dye fluorescence emission into higher-lying singlet states on dye laser performance has been discussed in a number of papers [1 - 5]. The dye *p*-phenylene-bis-(5-phenyl-2-oxazole) (POPOP) is of special interest since it has shown powerful laser emission in both liquid solution and in the vapour phase [6]. Since its efficiency in the vapour phase is less than that in solution, it can be asked whether excited state absorption effects play a significant role. Measurements of excited state absorption of this dye were performed, covering the visible and the near-UV portion of the spectrum. Measurement of excited state absorption characteristics in these different spectral regimes required application of various experimental methods. The techniques applied were based upon (1) bleaching of the ground state absorption, (2) probe beam techniques after intense N_2 laser excitation and (3) evaluation of the dependence of the small-signal gain on the pump intensity. In addition, time-resolved analysis of

the excited state absorption gave some indication of the magnitude of the triplet–triplet (T–T) absorption outside the fluorescence spectral range.

2. Experimental methods

The experimental procedure and the discussion of the experimental results are closely related to the simplified energy level diagram of a dye molecule as shown in Fig. 1. Only those processes which are taken into consideration in the following description of the experimental data evaluation are shown in Fig. 1. The energy level diagram is divided into the singlet system (S_0, S_1, S_n) and the triplet system (T_1, T_n). The respective population densities are N_0, N_1, N_n, N_{T_1} and N_{T_n}. Conservation of the total number N of molecules per volume requires the condition

$$N = N_0 + N_1 + N_n + \ldots + N_{T_1} + N_{T_n} \tag{1}$$

Absorption processes in the singlet and triplet manifolds can take place via absorption of pump light (index p) and via fluorescence radiation (index l). The respective absorption cross sections are shown in Fig. 1, with the notation essentially following the symbols introduced in refs. 4 and 7. Spontaneous decay will be considered in terms of the S_1 lifetime τ_1, and decay by stimulated emission will be considered in terms of the cross section σ_e.

In the spectral range of strong singlet absorption we applied both the absorption probe technique as discussed in more detail later and the intensity-dependent bleaching method for ground state absorption at the pump wavelength [8]. In agreement with previous results [2] the ratio $\sigma_{ap}^0 : \sigma_{ap}^1$ of the cross section of ground state absorption to that of excited state absorption was determined to be 2:1 at the N_2 laser wavelength of 337.1 nm. This data also served as a calibration for the excited state absorption measure-

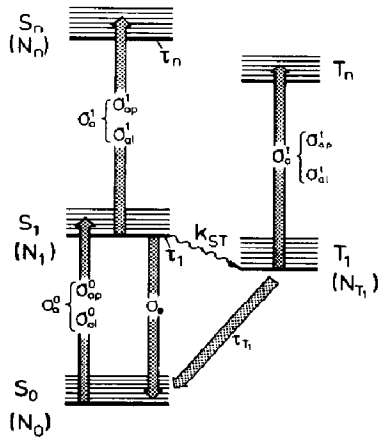

Fig. 1. A typical energy level diagram of dye singlet S_i and triplet T_i states: N_i, population densities; σ_i, cross sections; τ_i, decay times; k_{ST}, the intersystem crossing rate constant.

ments with the flash photolysis apparatus. In the spectral range of intense dye fluorescence, excited state absorption measurements were performed by both a probe beam technique using a tunable dye laser as the background source [1] and the method of small-signal gain measurement using the dependence of the amplified spontaneous emission on the pump intensity. In both procedures the small-signal gain g_0 is given by (see refs. 9 - 11)

$$g_0 = \sigma_e N\{I_p(1 - k_1^1) - k_1^0\}/(1 + I_p) \tag{2}$$

I_p denotes the pump power density $\tilde{I}_p$ divided by the saturation intensity $I_{ps} \approx \tau_1 \sigma_{ap}^0$. With $k_1^0 = \sigma_{a1}^0/\sigma_e$ and $k_1^1 = \sigma_{a1}^1/\sigma_e$, the unknown excited state absorption cross section σ_{a1}^1 can be determined from a plot of $g_0(1 + I_p)$ *versus* I_p [9].

By comparison of the fluorescence intensities obtained by successive irradiation of the right-hand side (I_1), the left-hand side (I_2) and the total length of the sample cell (I_{1+2}), the small-signal gain can be obtained as follows:

$$g_{exp} = \alpha - \beta = \frac{2}{L_0} \ln\left(\frac{I_{1+2}}{I_1} - 1\right) \tag{3}$$

where $\beta = (2/L_0) \ln (I_1/I_2)$. According to eqn. (2) the quantities α and β correspond to

$$\alpha \equiv \sigma_e N I_p(1 - k_1^1)/(1 + I_p)$$

and

$$\beta \equiv \sigma_{a1}^0 N/(1 + I_p)$$

Identification of α and β as measured by g_{exp} is based on the condition $g_{exp} \approx g_0$. We have studied this problem using a computer model [10]. Figure 2 shows some interesting results. The plot of g_{exp}/g_0 *versus* I_p for $\sigma_e N = 2\ cm^{-1}$ and various values of the ratio $D/l = a$ reveals that the assumption $g_{exp} \approx g_0$ is only justified if $I_p \gg 1$ and $D \gg l$. In the actual measurements, appropriate corrections were made with $D = 105$ mm and $l = 16$ mm.

In the spectral range outside the intense dye fluorescence region ($\lambda \leqslant 375$ nm and $\lambda \geqslant 520$ nm) excited state absorption was measured by conventional laser flash photolysis [12 - 14]. Intense N_2 laser pulses of 4 ns duration and approximately 4 mJ pulse energy served as the excitation source of the dye in solution. Transient absorption changes were monitored in a transverse observation geometry (Fig. 3) using a broad band spectrum from a 150 W xenon lamp. In order to improve the signal-to-noise ratio and to discriminate against the fluorescence of the dye, the probe light was synchronously pulsed for about 0.3 ms. This time allowed the observation of short-lived transients as well as of species decaying in the microsecond range. Experimental data were recorded using a 25 cm monochromator in conjunction with an RCA 4832 photomultiplier. The signals were displayed with a Tektronix 475 oscilloscope.

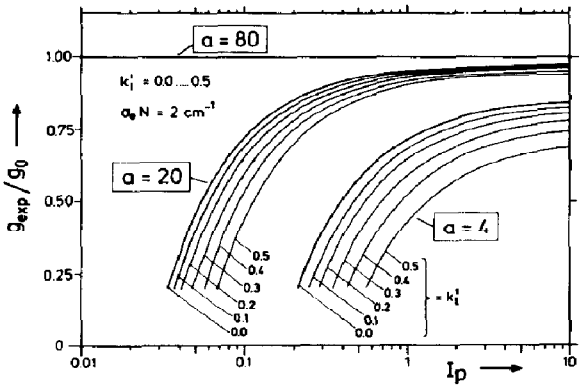

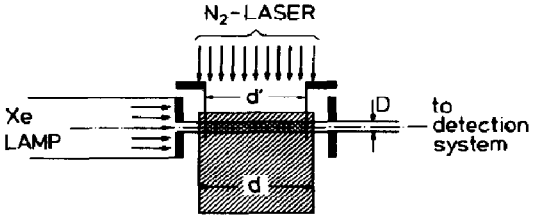

Fig. 2. A computer calculation of g_{exp}/g_0 *vs.* the pump intensity I_p for various k_i^1 values and three selected ratios for a of 4, 20 and 80, where a is the ratio of the detector distance D to the length l of the active medium.

Fig. 3. Experimental set-up for absorption measurement by laser flash photolysis with d = 10 mm (total absorption length), d' = 9 mm (N_2 laser excited length) and D = 1 mm (width of the xenon lamp probe beam).

For evaluation of the observed signals in terms of excited state absorption cross sections, the population density N_1 was derived from the measured change $\Delta E(\lambda_p)$ in extinction and the known ratio $\sigma_{ap}^0(\lambda_p)/\sigma_{ap}^1(\lambda_p)$ [2]. For $\lambda \neq \lambda_p$ an excited state absorption cross section $\sigma_{ap}^1(\lambda)$ can be calculated from the measured total change $\Delta E(\lambda)$ in extinction by means of the following equation:

$$\Delta E^1(\lambda) = \sigma_{ap}^1(\lambda) N_1 d'/\ln 10$$

$$= \Delta E(\lambda) + \frac{\sigma_{ap}^0(\lambda)}{\sigma_{ap}^0(\lambda_p)} \Delta E(\lambda_p) \left(\delta \frac{\sigma_{ap}^1(\lambda_p)}{\sigma_{ap}^0(\lambda_p)} - 1 \right)^{-1} \tag{4}$$

In eqn. (4) d' is the length of the N_2 laser excitation and $\delta = d'/d$ accounts for the different optical path length probed by the xenon lamp (Fig. 3).

The triplet state population density N_{T_1} at $t = t_0$ after the decay of the singlet excitation can be calculated from

$$N_{T_1}(t_0) = k_{ST} \int_0^{t_0} N_1(t') dt' \tag{5}$$

neglecting the decay of the triplet state which occurs on a microsecond time scale. With a given fluorescence quantum efficiency ϕ_f an upper limit for k_{ST} is given by

$$k_{ST} = \frac{1 - \phi_f}{\tau_1}$$

assuming fluorescence and intersystem crossing as the only deactivation pathways of the first excited singlet state S_1.

3. Experimental results

3.1. Fluorescence spectral range

Evaluation of eqn. (2) requires prior knowledge of $\sigma_{ap}^{0}(\lambda)$, $\sigma_{al}^{0}(\lambda)$ and $\sigma_e(\lambda)$. Figure 4 shows these cross sections for POPOP both in the vapour phase and in dioxan solution. The vapour phase data were taken from ref. 15. Both spectra were calibrated using the condition $\sigma_{ap}^{0max} \equiv \sigma_e^{max}$ according to ref. 16. Excited state absorption coefficients $k_1^1 = \sigma_{al}^1/\sigma_e$ were determined with the amplified spontaneous emission method for POPOP vapour at 382.5 nm and POPOP in dioxan solution at 411 nm. Both wavelengths correspond to the peaks of fluorescence emission as indicated in Fig. 4. Plots of $g^* = \alpha^* - \beta^* = g_0(1 + I_p) = \alpha(I_p) - \beta$ are shown in Fig. 5. The diagrams follow the characteristics of concentration dependence discussed in Section 2. Although the measured points for POPOP vapour show more scatter, the following values for k_1^1 can be obtained from the slopes of the various curves plotted in Fig. 5: $k_1^1 = 0.7 \pm 0.2$ (POPOP vapour); $k_1^1 = 0.36 \pm 0.1$ (POPOP in solution). The complete spectral dependence of $\sigma_{al}^1(\lambda) = k_1^1(\lambda)\sigma_e(\lambda)$, for POPOP vapour and for the dye in solution, is shown in Fig. 6. As in the range of ground state absorption at $\lambda_p = 337.1$ nm, POPOP vapour exhibits higher excited state absorption in the fluorescence spectral range than the same dye in solution. This may explain the usually observed lower laser performance [17] of a vapour laser compared with that of a liquid solution dye laser. However, the cross sections $\sigma_e(\lambda)$ for stimulated emission, the magnitude of which was confirmed from the data given in Fig. 4, are relatively high. Superradiant emission was observed from a transversely excited dye vapour cell at $T = 285$ °C (corresponding to a 5×10^{-5} M concentration) and $I_p = 0.5$ (corresponding to an N_2 laser pump power density of 4.1 MW cm^{-2}).

The σ_{al}^1 data of Fig. 6 reflect the shape of the fluorescence spectrum. In order to confirm that this spectral feature does not depend on the amplified spontaneous emission method applied, a few data points (marked by rectangular symbols) were measured with a conventional probe beam technique

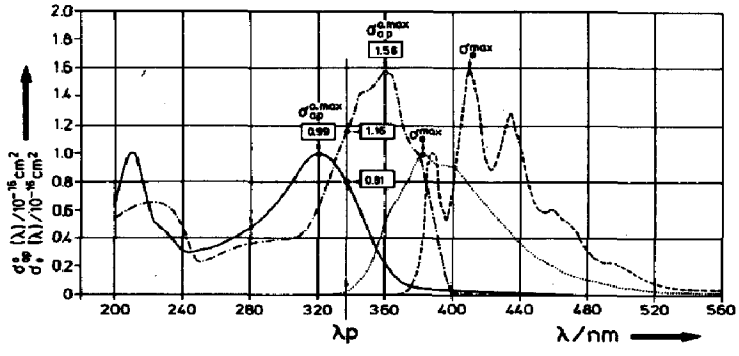

Fig. 4. Cross sections for ground state absorption ($\sigma_{ap}^{0}(\lambda)$) and stimulated emission ($\sigma_e(\lambda)$) for POPOP in dioxan solution and in the vapour phase: ——, σ_{ap}^{0}, POPOP vapour; ···, σ_e, POPOP vapour; ·—·—·, σ_{ap}^{0}, POPOP in dioxan; – – –, σ_e, POPOP in dioxan.

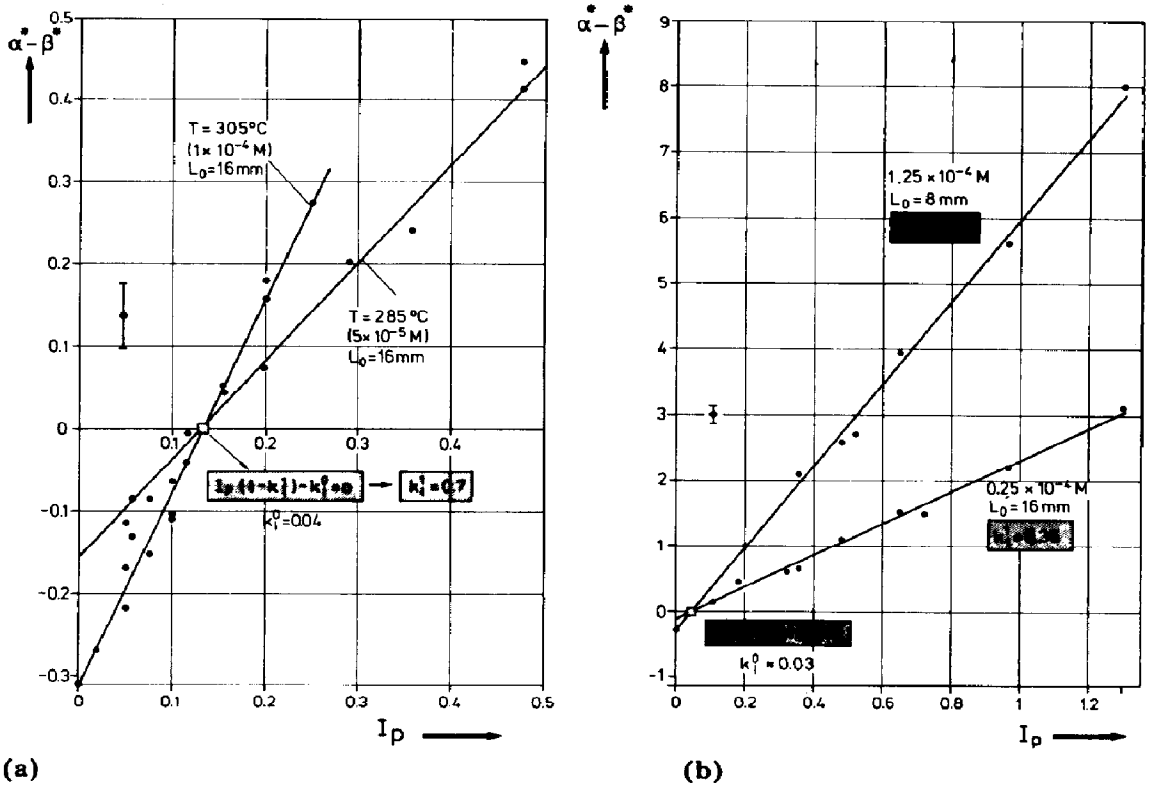

Fig. 5. Determination of the excited state absorption coefficients k_1^1 for (a) POPOP vapour and (b) POPOP in dioxan for various concentrations at the peak of the fluorescence spectra. At the concentration 1.25×10^{-4} M the active length had to be reduced to L_0 = 8 mm to suppress onset of laser oscillation.

using a dye laser as the probing light source. Such measurements lead to comparable results. Figure 6 shows that the excited state absorption cross section σ_{a1}^1 does not exceed 0.4×10^{-16} cm^2 in the spectral range of optimum laser performance for POPOP in liquid solution.

3.2. Spectral ranges $\lambda \leqslant 375$ nm and $\lambda \geqslant 520$ nm

Figure 7 shows typical oscilloscope traces obtained with the laser flash photolysis apparatus. The lower traces represent the total signal of both absorption change and fluorescence, which have to be corrected for an eventual fluorescence contribution. The fluorescence itself at the given wavelength is displayed in the upper trace and was obtained by blocking the probe light. To illustrate the evaluation procedure Fig. 8 shows four spectra in the range 310 - 375 nm, with the lower part of the figure depicting the primarily measured changes in extinction ΔE and the upper part showing the finally obtained cross sections $\sigma_a^1(\lambda)$ by application of eqn. (4). The data points shown by open circle symbols represent the ΔE values measured at the time of maximum excited state absorption. Triplet–triplet absorption

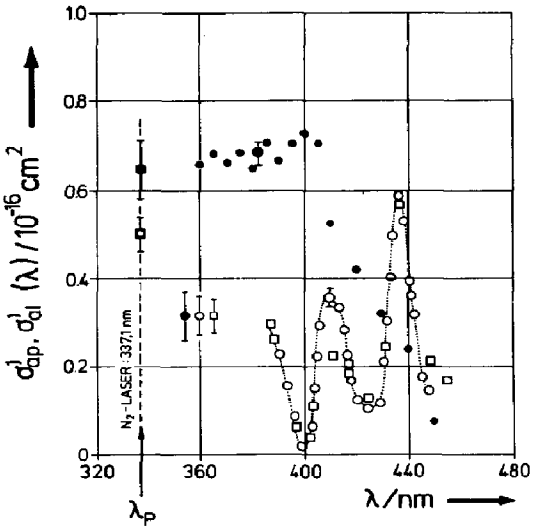

Fig. 6. Compilation of excited state absorption cross sections $\sigma^1_{ap}(\lambda)$ and $\sigma^1_{al}(\lambda)$ for POPOP vapour (●, ■) and POPOP in dioxan (○, □, ◻): □, ■, data points obtained by a laser probe beam; ○, ●, data points obtained by the amplified spontaneous emission technique.

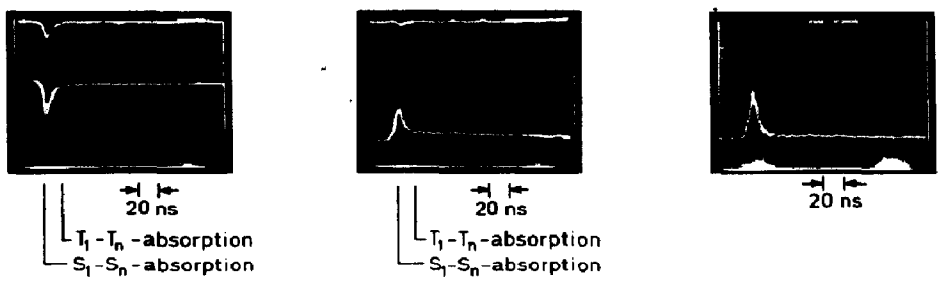

(a) (b) (c)

Fig. 7. Typical oscilloscope traces showing the primarily monitored extinction changes ΔE (lower traces) and the eventual fluorescence emission (upper traces): (a) λ = 360 nm, $\sigma^0_{ap} > \sigma^1_{ap}$; (b) λ = 575 nm, $\sigma^1_{ap} > \sigma^0_{ap} = 0$; (c) λ = 720 nm, $\sigma^1_{ap} > \sigma^0_{ap} = 0$.

data were measured after decay of the fluorescence (Fig. 7) and were evaluated in terms of cross sections using eqn. (5) and

$$\Delta E^t = \Delta E + \sigma^0_a N_{T_1} d'/\ln 10 = \sigma^t_a N_{T_1} d'/\ln 10 \qquad (6)$$

With τ_1 = 1.2 ns, ϕ_f = 0.93 [18] and $N_1/N \approx 20\%$, N_{T_1} can be estimated to be approximately $N_1/3$. This high triplet population is a consequence of the long lifetime τ_{T_1} in the microsecond range of the triplet state T_1, leading to an accumulation of molecules in the triplet state via intersystem crossing during the duration of the excitation pulse.

For the long-wavelength range $\lambda \geqslant 520$ nm no ground state absorption ($S_0 \rightarrow S_1$) has to be considered. Therefore the measured extinction changes correspond directly to $S_1 \rightarrow S_n$ and $T_1 \rightarrow T_n$ absorption. Figure 9 depicts the

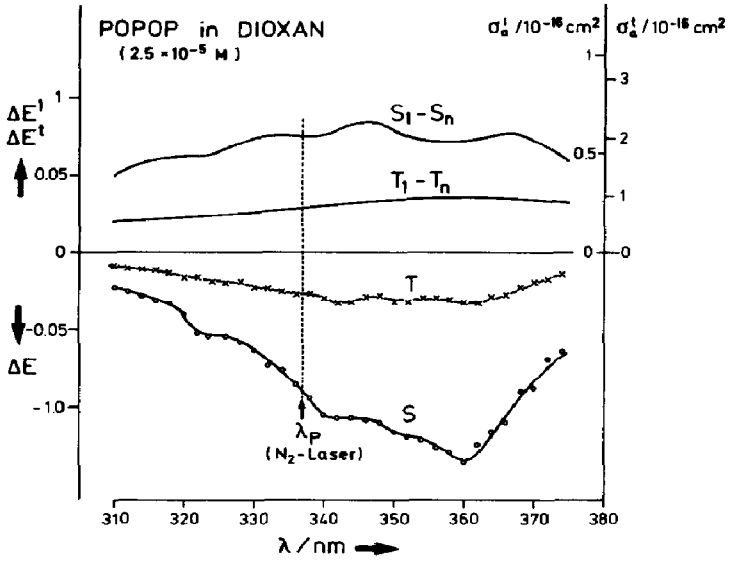

Fig. 8. Evaluation of laser flash photolysis data in the wavelength range 310 - 375 nm. The lower part shows total singlet absorption S and triplet absorption T with data taken at times indicated in Fig. 7. After correction for ground state depletion (eqns. (4) and (6)), values for extinction changes ΔE^1 and ΔE^t and finally cross sections σ_a^1 and σ_a^t were obtained and are plotted in the upper part of the figure.

wavelength dependences of ΔE^1 (S_1–S_n absorption) and ΔE^t (T_1–T_n absorption) as derived from the time-resolved evaluation of the oscilloscope traces shown in Fig. 7. The structure of the S_1–S_n spectrum is much more pronounced here than in the short-wavelength region ($\lambda \leqslant 375$ nm), giving clear evidence for the vibronic splitting in the corresponding excited singlet state. From the extinction changes ΔE^1 and ΔE^t absorption cross sections σ_a^1 and σ_a^t were determined by applying the population densities N_1 and N_{T_1} used in the wavelength range $\lambda \leqslant 375$ nm. At $\lambda = 724$ nm (Fig. 9) $\sigma_a^1 = 2 \times 10^{-16}$ cm^2,

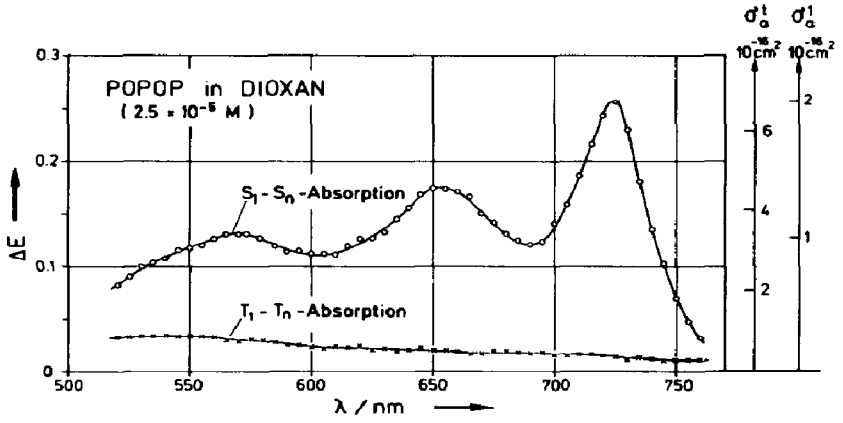

Fig. 9. Extinction changes due to S_1–S_n and T_1–T_n absorption in the spectral range 520 - 760 nm.

a value which is even higher than $\sigma_a^0 = 1.55 \times 10^{-16}$ cm^2 at $\lambda = 360$ nm, the peak of the $S_0 \rightarrow S_1$ absorption of POPOP in solution. The triplet spectrum shown in Fig. 9 is in agreement with experimental results given previously [19].

4. Discussion

The excited state absorption data obtained for the various spectral regions are summarized in Fig. 10. Figures 8 and 9 indicate the relatively constant splitting of the electronic singlet levels into a vibronic substructure denoted by v_i^1, v_i^2 and v_i^3 with $i = 0, 1, 2,...$ Energy difference Δv_i values in the range $\Delta v_i = 0.2$ eV were determined experimentally. The well-resolved vibronic substructure facilitates the characterization of a POPOP energy level diagram, including the higher-lying singlet states S_2 and S_3 as shown in Fig. 10. The level S_2 was located relative to S_1 by means of the long-wavelength absorption spectrum given in Fig. 9. With an energy position for S_1 of 3.2 eV relative to S_0, the vibronic substructure v_2^1, v_2^2 and v_2^3 comprises the energy range from 4.9 to 5.3 eV. The observed absorption peak at 235 nm shown in Fig. 4 can tentatively be attributed to an $S_0 \rightarrow S_2(v_2^3)$ transition. The identification of S_3 in the energy range from 5.90 to 6.25 eV is based upon the assignment of the observed excited state absorption peak at 435 nm (see Fig. 6) to an $S_2 \rightarrow S_3(v_3^2)$ transition under the assumption that the $S_1 \rightarrow S_3(v_3^1)$ transition is missing in Fig. 6, since it could neither be observed by the

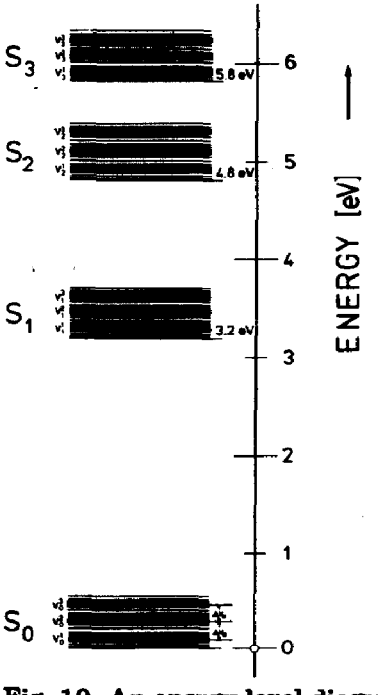

Fig. 10. An energy level diagram for the POPOP singlet states.

amplified simultaneous emission method because of a too small σ_e value nor by the flash photolysis method because the fluorescence was already too high. The spectral position of S_2 is in good agreement with other experimental observations using electron energy loss spectroscopy [20] for the identification of unknown higher-lying singlet levels. Low excited state absorption at the centre of the S_1 fluorescence around 410 nm was confirmed using an N_2-laser-pumped POPOP laser; a high loss cavity with 100% and 4% reflectors allowed laser operation only in the wavelength range of low excited state absorption losses, *i.e.* 400 - 425 nm. Although the cross section for stimulated emission σ_e exceeds σ_{a1}^1 at 435 nm, the described dye laser could not be operated at this wavelength in liquid solution. Under comparable conditions of vapour density and cavity properties laser operation in the vapour phase was also restricted to the centre peak of the vapour fluorescence.

In conclusion, it has been shown that measurements of excited state absorption cross sections together with the known S_0–S_1 data allow the construction of a refined energy level diagram of a typical laser dye. Such a diagram reveals the interesting fact that in the case of POPOP S_1–S_3 absorption and not S_1–S_2 absorption is most probably the process of fluorescence quenching in the wavelength range of dye laser operation.

References

1 E. Sahar and I. Wieder, *Chem. Phys. Lett., 23* (1973) 518.
2 E. Sahar and I. Wieder, *IEEE J. Quantum Electron., 10* (1974) 612.
3 E. Sahar and D. Treves, *IEEE J. Quantum Electron., 13* (1977) 962.
4 O. Teschke, A. Dienes and J. R. Whinnery, *IEEE J. Quantum Electron., 12* (1976) 383.
5 P. R. Hammond, *Appl. Opt., 18* (1979) 536.
6 P. W. Smith, *Opt. Acta, 23* (1976) 901.
7 W. Heudorfer and G. Marowsky, *Appl. Phys., 17* (1978) 181.
8 M. Hercher, *Appl. Opt., 6* (1967) 947.
9 G. Marowsky, *IEEE J. Quantum Electron., 16* (1980) 49.
10 G. Marowsky and F. K. Tittel, *Appl. Opt., 19* (1980) 138.
11 C. V. Shank, *Rev. Mod. Phys., 47* (1975) 649.
12 J. R. Novak and M. W. Windsor, *J. Chem. Phys., 47* (1967) 3075.
13 A. Müller, *Z. Naturforsch., Teil A, 23* (1968) 946.
14 H. Schomburg, *Dissertation*, Göttingen, F.R.G., 1975.
15 B. Steyer and F. P. Schäfer, *Appl. Phys., 7* (1975) 113.
16 In F. P. Schäfer (ed.), *Dye Lasers*, Springer, Berlin, 2nd edn., 1977.
17 P. W. Smith, P. F. Liao, C. V. Shank and T. K. Gustafson, *Appl. Phys. Lett., 25* (1974) 144.
18 I. Berlman, *Handbook of Fluorescence Spectra of Aromatic Molecules*, Academic Press, New York, 1971.
19 T. G. Pavlopoulos and P. R. Hammond, *J. Am. Chem. Soc., 96* (1974) 6568.
20 H. W. Hertel, I. V. Hermann and G. Marowsky, *Appl. Phys., 15* (1978) 185.